AJAPAS

African Journal of Advanced Pure and Applied Sciences (AJAPAS)

Online ISSN: 2957-644X
Volume 4, Issue 3, 2025
Page No: 55-62
Website: https://aaasjournals.com/index.php/ajapas/index

ISI 2025: 1.126 SJIFactor 2024: 6.752 معامل التأثير العربي: 1.62

Implementation of ZVS interleaved booster converter in Electric vehicles with reduced THD

Abubaker Emheisen [1 *], Mustafa Emheisen [2]
[1,2] Electrical and Electronic Engineering Department, Bani Waleed University, Libya

تنفيذ محول معزز متداخل ZVS في المركبات الكهربائية مع تقليل THD

أبوبكر إمحيسن [1*]، مصطفى إمحيسن [2]
[2،1] قسم الهندسة الكهربائية والإلكترونية، جامعة بني وليد، ليبيا

[*]*Corresponding author: aemheisen@gmail.com*

Received: May 19, 2025	Accepted: July 05, 2025	Published: July 13, 2025

Abstract

With the increase in global infrastructure, electric vehicles (EVs) are the replacement for many conventional transportation. In recent years, there has been significant development in EV technology to increase efficiency and reduce the THD of the machine. This paper proposes a new converter topology ZVS interleaved booster converter, for traction purposes when connected to the smart grid. The analysis and performance with complete modes of operation is been discussed with a graphical representation of outputs of the DC machine. The modeling and analysis are done using MATLAB Simulink.

Keywords: ZVS, Electric vehicles, THD.

الملخص

مع ازدياد البنية التحتية العالمية، أصبحت المركبات الكهربائية بديلاً للعديد من وسائل النقل التقليدية. في السنوات الأخيرة، شهدت تكنولوجيا المركبات الكهربائية تطوراً ملحوظاً لزيادة كفاءتها وتقليل التشوه التوافقي الكلي (THD). تقترح هذه الورقة البحثية طوبولوجياً جديدة لمحول التعزيز المتداخل ZVS، لأغراض الجر عند توصيله بالشبكة الكهربائية الذكية. تمت مناقشة التحليل والأداء مع جميع أوضاع التشغيل من خلال تمثيل بياني لمخرجات آلة التيار المستمر. تم إجراء النمذجة والتحليل باستخدام MATLAB Simulink.

الكلمات المفتاحية: ZVS، المركبات الكهربائية، THD.

Introduction

A general hybrid electrical vehicle utilizes huge battery banks with large capacities. The discharging characteristics of the battery are also very much higher efficient that the conventional technologies. The application of such traction drives in an electrical bus system is a challenge where the power quality of the grid system has to be maintained. We consider a smart grid where EV is used as a traction element or for transportation. Application of smart grids ensures the reliability of power and maintains the affordability of the devices for the operation. A simple smart grid with EV application is shown in Figure 1.

Figure 1 defines the utilization of power electronics in an EV with boost capabilities with a ZVS interleaved booster converter with reduced THD (Total Harmonic Distortion). The machine used to drive the load is a three-phase induction machine. This plug-in electric vehicle uses a high-voltage battery to charge it through an external supply from the smart grid. There are two stages in this converting operation: the rectifier stage, where the battery gets charged up, and an inversion stage, where the load, ie. An induction motor is operated from the battery supply of power. A complete conversion block diagram is given in Figure 2.

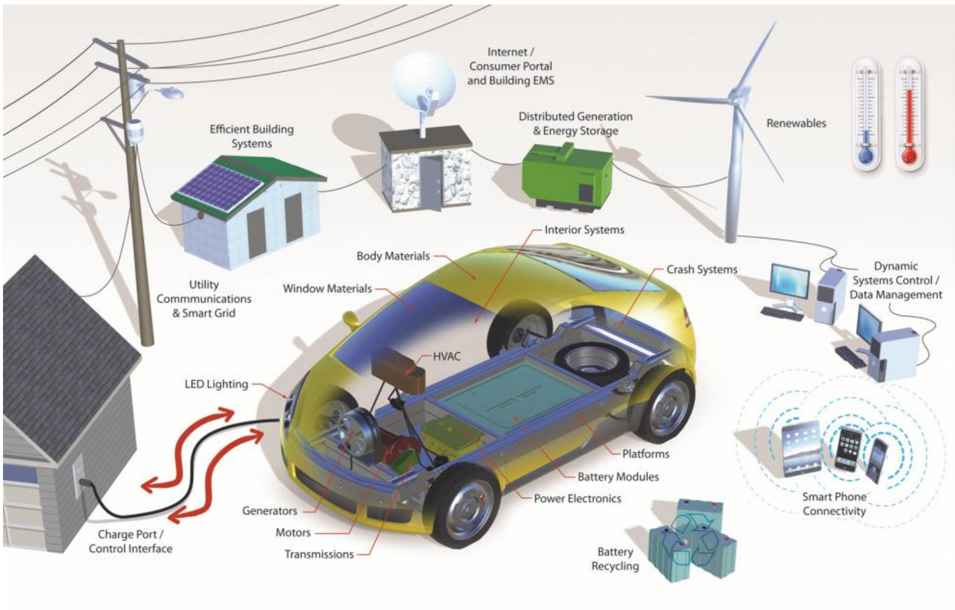

Figure 1: Electric vehicle in Smart grid application**.**

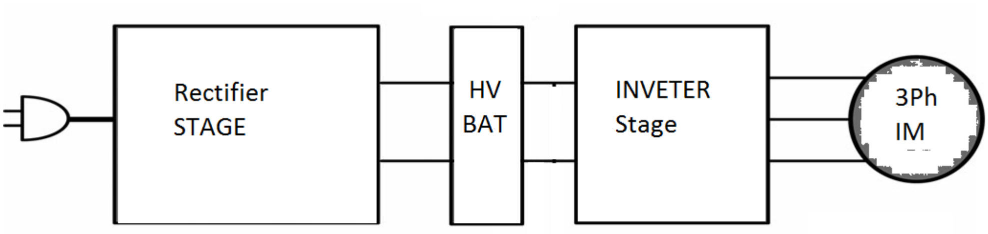

Figure 2: Block diagram of the converter.

In the interleaved booster converter, there is a continuous current conduction mode (CCM) basically used to realize Power factor correction (PFC). The rectifier stage includes a Diode Bridge Rectifier (DBR) to converter AC into rippled DC fed to a double booster converter with two boosting inductors. For the boosting operation MOSFETs are used due to high switching frequency operation. The output of the converter has a very high gain around 4 times of the input DC voltage from the DBR. The schematic of the interleaved PFC booster converter is shown in Figure3 below.

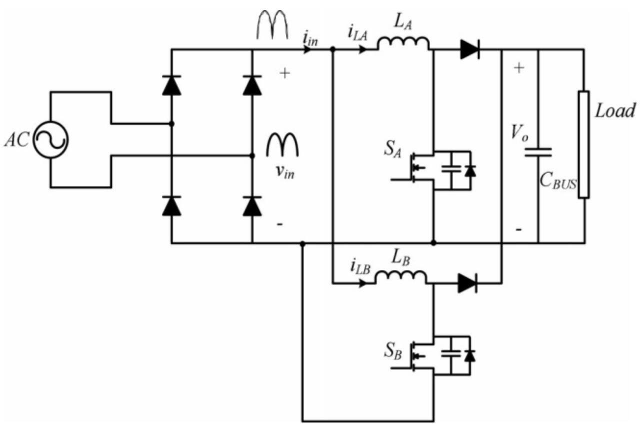

Figure 3: Interleaved PFC booster converter.

With the switching of the power electronic switches MOSFETs with a controlled duty ratio the output boost voltage is controlled. Zero voltage switching (ZVS) is the secondary circuit that has to be implemented which further includes in the interleaved booster converter. An auxiliary circuit with PWM (Pulse width Modulation) ZVS operation is basically of two types, one of them is resonant and the other is non-resonant. The ZVS with auxiliary circuit with interleaved PFC converter is shown in Figure 4.

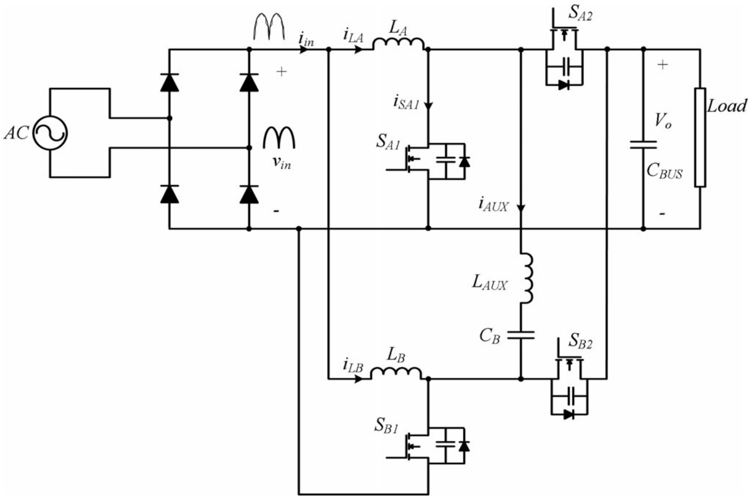

Figure 4: Auxiliary ZVS circuit with interleaved booster converter.

The auxiliary circuit is a combination of two MOSFET switches and a series auxiliary passive element combination with an inductor and a capacitor.

Analysis of ZVS Interleaved Booster Converter

The ZVS operation is done with change in the switching states for every 180^0 phase shift to reduce the ripple in the current of the converter. The auxiliary circuit will be in resonance as there is a high frequency inductor with a blocking capacitor in order to eliminate DC currents increment in the main switches of the converter. The switching states of the all the four MOSFETs is as below in Figure 5.

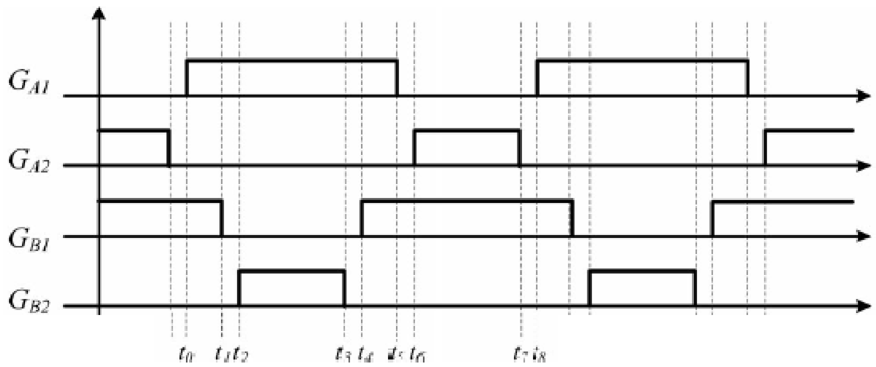

Figure 5: Switching states of MOSFETs.

The operating modes are explained below at different instants of time.

Mode I:

This is mode is between the time instants as $t0 < t < t1$ where the switches SA1 and SB1 will be in ON state. The current through the switch is given as

$$i_{SA1}(t) = I_V - I_{\mathrm{Aux},p} - \frac{v_{\mathrm{in}}}{L_A}(t - t_0)$$

Mode II:

This mode is between the tine intervals $t1 < t < t2$ where the auxiliary circuit is in operation and the current through the aux circuit is given as

$$i_{\mathrm{AUX}}(t) = I_{\mathrm{Aux},p} - \frac{V_o}{2(t_2 - t_1)L_{\mathrm{AUX}}}(t - t_1)^2$$

Mode III:

This mode is between t2 < t < t3 the switch SB2 is turned ON under ZVS when both the capacitors of SB1 and SB2 are fully charged. The current through the auxiliary circuit at this mode is given as

$$i_{\mathrm{AUX}} = I_{\mathrm{Aux},p} - \frac{V_o}{2L_{\mathrm{AUX}}}t_d - \frac{V_o}{L_{\mathrm{AUX}}}(t - t_2)$$

Mode IV:
During this time state (t3 < t < t4) the output capacitor SB2 is discharging and the output capacitor SB1 is charging to a value of Vo. The auxiliary current is

$$i_{\mathrm{AUX}}\,(t) = I_{\mathrm{Aux},p} + \frac{3V_o}{2L_{\mathrm{AUX}}} t_d$$

Mode V:
The switches SA1 and SB1 are in ON state during this mode $t4 < t < t5$ where the voltage across the aux inductor is zero and the current remains constant.

$$i_{LA}(t) = I_V + \frac{v_{\mathrm{in}}}{L_A}(t - t_0)$$

Mode VI:
The output capacitor of SA2 is discharging from Vo and output capacitor of SA1 is charging to Vo during $t5 < t < t6$.

$$i_{\mathrm{AUX}}\,(t) = -I_{\mathrm{Aux},p} + \frac{V_o}{2t_d L_{\mathrm{AUX}}}(t - t_5)^2$$

Mode VII:
During this time interval $t6 < t < t7$ the voltage across the aux inductor is Vo so the current through the aux circuit is given as

$$i_{\mathrm{AUX}}\,(t) = -I_{\mathrm{Aux},p} + \frac{V_o}{2L_{\mathrm{AUX}}} t_d + \frac{V_o}{L_{\mathrm{AUX}}}(t - t_6)$$

Mode VIII:
In this operating mode ie., between $t7 < t < t8$ the output capacitor of SA2 is charging to Vo and the output capacitor of SA1 is discharging from Vo. The aux current at this instant of time is given as

$$i_{\mathrm{AUX}}(t) = -I_{\mathrm{Aux},p} + \frac{V_o}{2L_{\mathrm{AUX}}} t_d$$

Simulink Design and Outputs
The complete analysis is carried out in MATLAB Simulink. The design of the smart grid and ZVS interleaved booster converter is shown below in Figures 5 and 6.

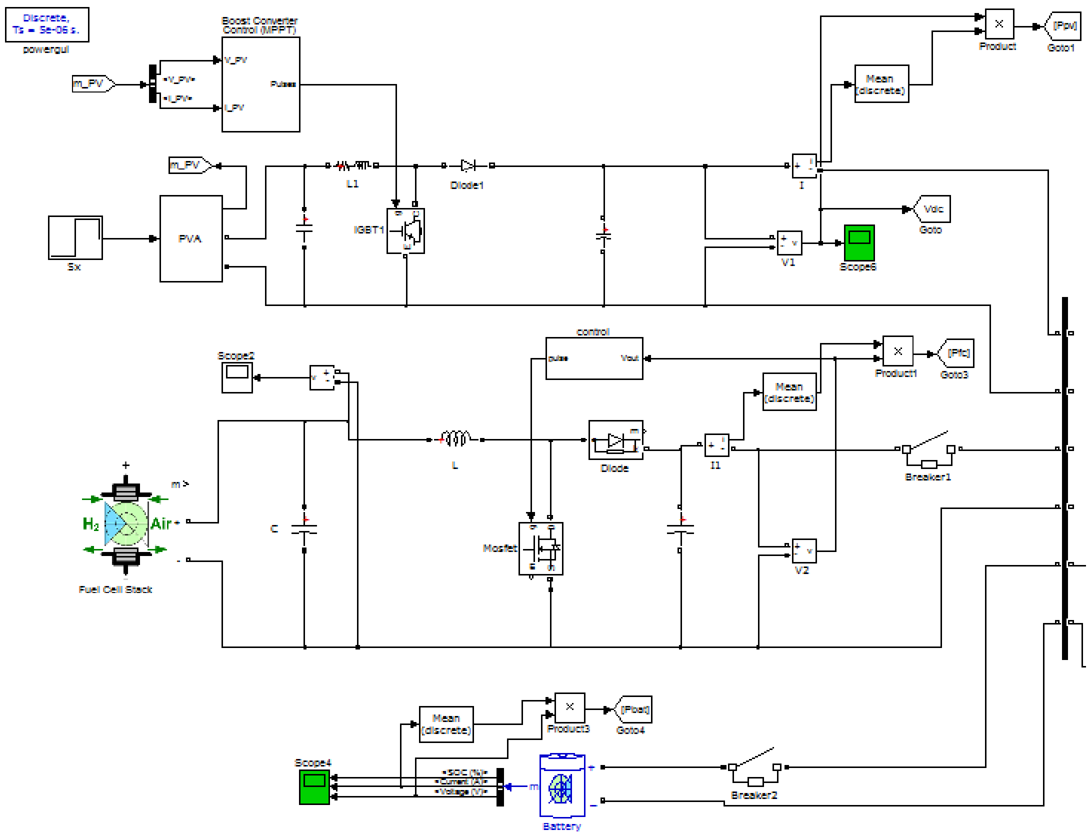

Figure 6: Smart grid Simulink design.

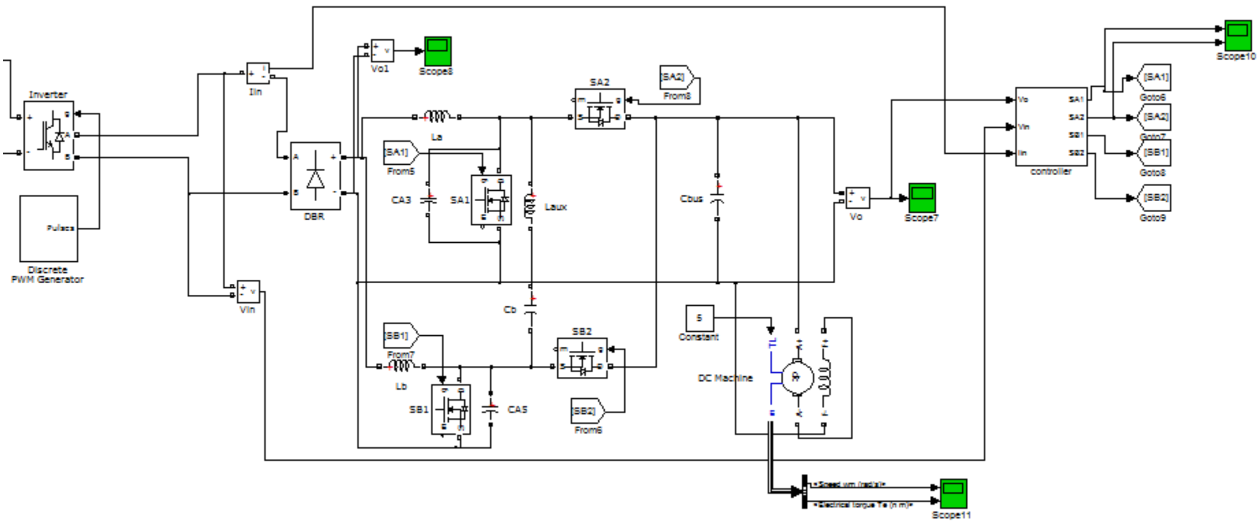

Figure 7: ZVS interleaved booster converter with EV application.

The smart grid is a combination of three different renewable sources, which include PVA, a Fuel cell and a battery. All three sources are connected through DC-DC converters to a DC bus. The voltage of the DC bus is shown in Figure 8, defining the voltage at approximately 400V. The DC bus. After the DC bus an inverter is utilized to convert DC to AC voltage. The AC voltage is now fed to the ZVS interleaved booster converter.

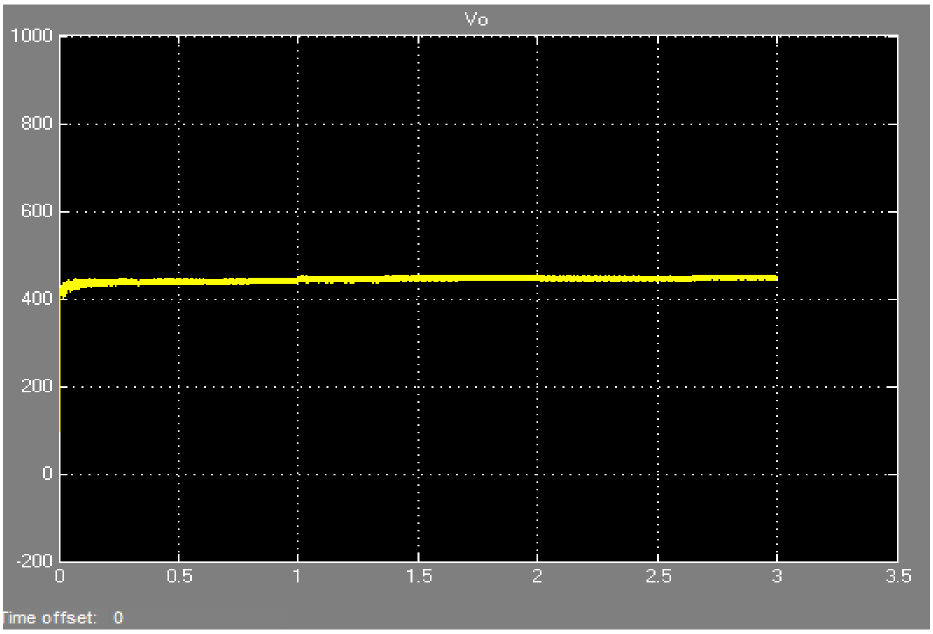

Figure 8: Voltage of DC bus.

Power outputs of each source are shown in Figure 9 where the Ppv is blue, Pfc is green and the red is the battery power Pbat in charging state. The power of the battery is in negative as the state of charge if the battery is 40% tending to charge from the renewable sources available.

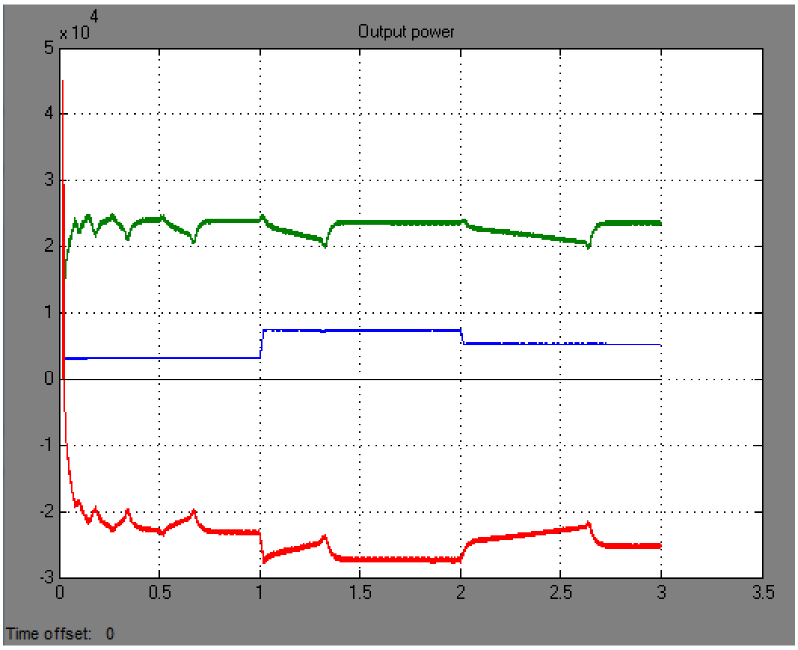

Figure 9: Output power of sources.

With further connections to the system, a full bridge IGBT inverter is attached to the DC bus employing PWM technique to convert DC to AC voltage. The ZVS interleaved booster converter with DC machine is attached to the inverter for a boosted DC voltage fed to the DC motor. The voltage output of the interleaved booster converter can be seen in Figure 10 with less ripple during load conditions.

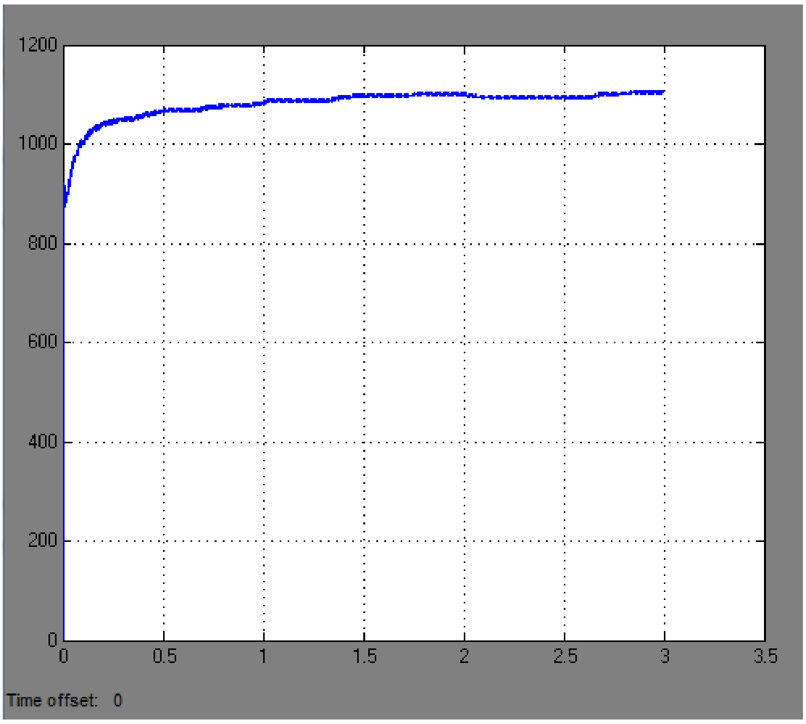

Figure 10: DC output voltage of ZVS interleaved booster converter.

The output boosted voltage of 1100V from the output of the converter is now is fed to the DC motor and the operating characteristics are displayed with respect to time in Figure 11. The graph shows the speed (w rad/sec) of the DC machine compared to the electromagnetic torque (Te Nm) where the torque is very much high during the start to overcome the inertia. The speed initializes from 0 rad/sec and gradually settles at 650 rad/sec.

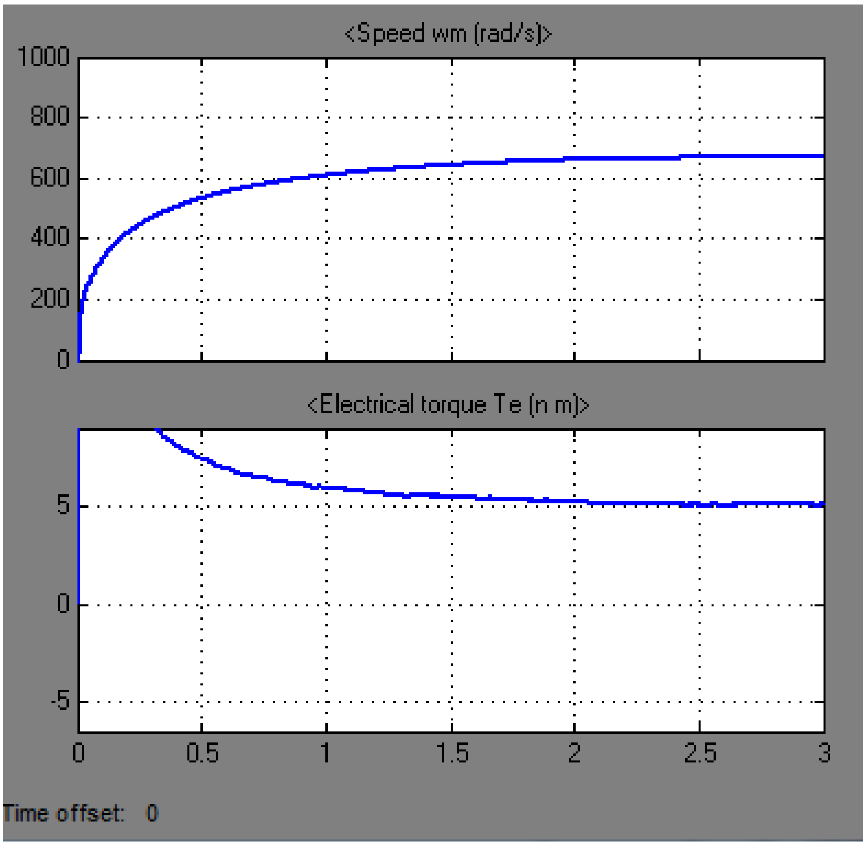

Figure 11: Characteristics of a DC motor.

Conclusion

In the above design and analysis of the ZVS interleaved booster converter is studied with complete graphs of the outputs of each source and load characteristic are explained in the paper. The output DC voltage of the ZVS converter has a gain of about 2.75 times the input voltage. Application of the EV in the smart grid with different renewable energy resources has been successfully implemented with lesser harmonics and ripples.

References

[1] M. Young, The Technical Writer's Handbook. Mill Valley, CA: University Science, 1989.

[2] T. Nussbaumer, M. Baumann, and J. W. Kolar, "Comparative evaluation of modulation methods of a three-phase buck + boost PWM rectifier. Part II: Experimental verification," Power Electron., IET, vol. 1, no. 2, pp. 268–274, Jun. 2008.

[3] T. Nussbaumer and J. W. Kolar, "Comparison of 3-phase wide output voltage range PWM rectifiers," IEEE Trans. Ind. Electron., vol. 54, no. 6, pp. 3422–3425, Dec. 2007.

[4] R. Giral, L. Martinez-Salamero, and S. Singer, "Interleaved converters operation based on CMC," IEEE Trans. Power Electron., vol. 14, no. 4, pp. 643–652, Jul. 1999.

[5] T.-W. Kim, H.-S. Kim, and H.-W. Ahn, "An improved ZVT PWM boost converter," in Proc. Conf. Rec. IEEE Power Electron. Spec. Conf., 2000, pp. 615–619.

[6] N. Jain, P. Jain, and G. Joos, "A zero voltage transition boost converter employing a soft switching auxiliary circuit with reduced conduction losses," IEEE Trans. Power Electron., vol. 19, no. 1, pp. 130–139, Jan. 2004.

[7] M. L. Martins, H. A. Grundling, H. Pinheiro, J. R. Pinheiro, and H. L. Hey, "A ZVT PWM boost converter using auxiliary resonant source," in Proc. Conf. Rec. IEEE Appl. Power Electron. Conf., 2002, pp. 1101–1107.

[8] Wang, Y., Chen, K.S., Mishler, J., Cho, S.C., Adroher, X.C.: 'A review of polymer electrolyte membrane fuel cells: technology, applications, and needs on fundamental research', Appl. Energy, 2011, 88, (4), pp. 981–1007

[9] Dursun, E., Kilic, O.: 'Comparative evaluation of different power management strategies of a standalone PV/wind/PEMFC hybrid power system', Electr. Power Energy Syst., 2012, 34, (1), pp. 81–89

[10] Onar, O.C., Uzunoglu, M., Alam, M.S.: ‘Modelling, control and simulation of an autonomous wind turbine/photovoltaic/fuel cell/ultra-capacitor hybrid power system’, J. Power Sources, 2008, 185,(2), pp. 1273–1283

[11] Ahmed, N.A., Miyatake, M., Al-Othman, A.K.: ‘Power fluctuations suppression of stand-alone hybrid generation combining solar photovoltaic/wind turbine and fuel cell systems’, Energy Convers. Manage., 2008, 49, (10), pp. 2711–2719

[12] Ipsakis, D., Voutetakis, S., Seferlis, P., Stergiopoulos, F., Elmasides, C.: ‘Power management strategies for a standalone power system using renewable energy sources and hydrogen storage’, Int. J. Hydrog. Energy, 2009, 34, (16), pp. 7081–7095

[13] Zhou, W., Lou, C., Li, Z., Lu, L., Yang, H.: ‘Current status of research on optimum sizing of standalone hybrid solar–wind power generation systems’, Appl. Energy, 2010, 87, (2), pp. 380–389

[14] Tofighi, A., Kalantar, M.: ‘Power management of PV/battery hybrid power source via passivity-based control’, Renew. Energy, 2011, 36, (9), pp. 2440–2450